energies

MDPI

Review

Application and Challenge of High-Speed Pumps with Low-Temperature Thermosensitive Fluids

Beile Zhang [1], Ben Niu [1], Ze Zhang [1,2], Shuangtao Chen [1,2], Rong Xue [1,2] and Yu Hou [1,2,*]

[1] School of Energy and Power Engineering, Xi'an Jiaotong University, Xi'an 710049, China; zbeile@stu.xjtu.edu.cn (B.Z.); niu_c@stu.xjtu.edu.cn (B.N.); zhangze@xjtu.edu.cn (Z.Z.); stchen.xjtu@mail.xjtu.edu.cn (S.C.); xuerong@mail.xjtu.edu.cn (R.X.)

[2] MOE Key Laboratory of Cryogenic Technology and Equipment, Xi'an Jiaotong University, Xi'an 710049, China

* Correspondence: yuhou@mail.xjtu.edu.cn

Abstract: The rapid development of industrial and information technology is driving the demand to improve the applicability and hydraulic performance of centrifugal pumps in various applications. Enhancing the rotational speed of pumps can simultaneously increase the head and reduce the impeller diameter, thereby reducing the pump size and weight and also improving pump efficiency. This paper reviews the current application status of high-speed pumps using low-temperature thermosensitive fluids, which have been applied in fields such as novel energy-saving cooling technologies, aerospace, chemical industries, and cryogenic engineering. Due to operational constraints and thermal effects, there are inherent challenges that still need to be addressed for high-speed pumps. Based on numerical simulation and experimental research for different working fluids, the results regarding cavitation within the inducer have been categorized and summarized. Improvements to cavitation models, the mechanism of unsteady cavity shedding, vortex generation and cavitation suppression, and the impact of cavitation on pump performance were examined. Subsequently, the thermal properties and cavitation thermal effects of low-temperature thermosensitive fluids were analyzed. In response to the application requirements of pump-driven two-phase cooling systems in data centers, a high-speed refrigerant pump employing hydrodynamic bearings has been proposed. Experimental results indicate that the prototype achieves a head of 56.5 m and an efficiency of 36.1% at design conditions (n = 7000 rpm, Q = 1.5 m^3/h). The prototype features a variable frequency motor, allowing for a wider operational range, and has successfully passed both on/off and continuous operation tests. These findings provide valuable insights for improving the performance of high-speed refrigerant pumps in relevant applications.

Keywords: high-speed centrifugal pump; thermosensitive fluid; cavitation; thermal effect; hydrodynamic bearing

Citation: Zhang, B.; Niu, B.; Zhang, Z.; Chen, S.; Xue, R.; Hou, Y. Application and Challenge of High-Speed Pumps with Low-Temperature Thermosensitive Fluids. *Energies* **2024**, *17*, 3732. https://doi.org/10.3390/en17153732

Academic Editor: Alessia Arteconi

Received: 24 June 2024
Revised: 20 July 2024
Accepted: 26 July 2024
Published: 29 July 2024

1. Introduction

Centrifugal pumps are the most prevalent type of pump due to their stable output, compact structure, and high reliability. These characteristics make them widely used in many applications such as industrial, agricultural, military, and domestic fields [1,2]. To achieve the demands of complex operating environments and conditions, there is a growing need for centrifugal pumps to develop in the direction of miniaturization, having a high head and high efficiency, and being lightweight. This is particularly critical in military applications [3] and aerospace systems [4], where equipment must reliably operate under all or specific operating conditions.

By increasing the pump rotational speed under identical inlet conditions, it is possible to achieve a higher head and simultaneously reduce the impeller diameter, overall dimension, weight, and manufacturing costs. The specific speed, $n_q = nQ^{0.5}/H^{0.75}$, is a dimensionless parameter that evaluates a pump's performance across different design

conditions, which depends on the flow rate Q, head H, and rotational speed n. When the flow rate and head are constant, increasing the rotational speed enhances the specific speed n_q. For low-specific-speed centrifugal pumps, a higher specific speed number usually leads to better impeller efficiency. In multistage centrifugal pumps, increased speed can augment the pressure-boosting capacity of each stage, thereby minimizing interstage losses and enhancing pump efficiency [5].

As fluid machinery used for liquid transport or pressurization, centrifugal pumps are applicable not only for water and aqueous solutions [6–12] but also for low-temperature thermosensitive fluids such as refrigerants and cryogens. In fields such as new energy-saving cooling technologies, aeronautics and astronautics industries, chemical industries, and cryogenic engineering, centrifugal pumps designed for thermosensitive fluids play an essential role. Typical engineering application situations are shown in Figure 1. In most of these applications, there are high standards for pump performance and reliability. Increasing the pump rotational speed emerges as an effective strategy to fulfill these stringent requirements.

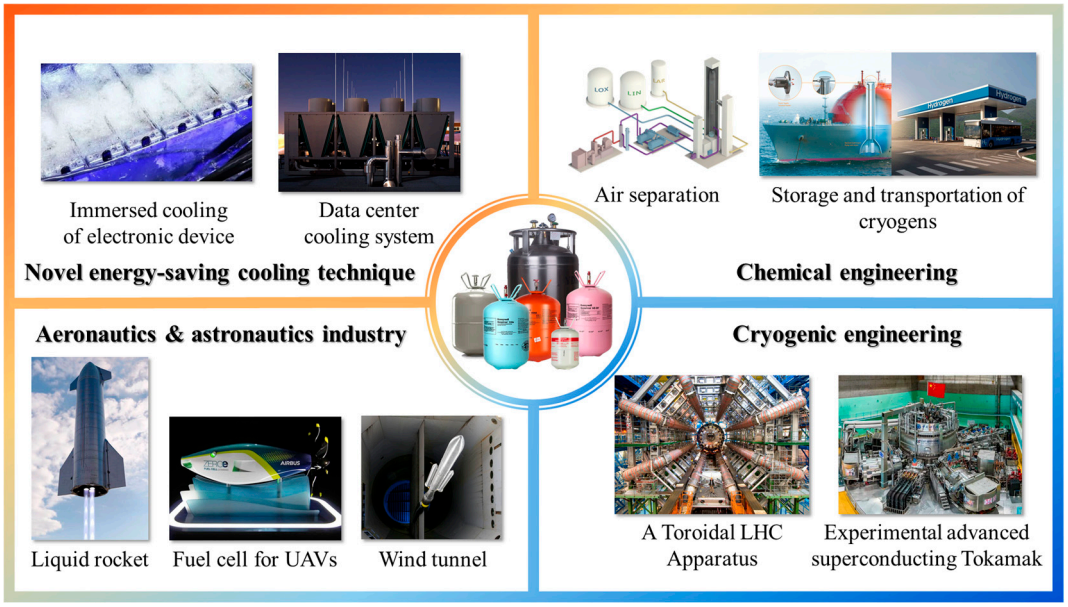

Figure 1. Typical applications of centrifugal pumps with low-temperature thermosensitive fluids.

However, several engineering challenges must be addressed before high-speed pumps can be widely applied, especially as rotational speeds increase. One significant issue is cavitation, which occurs when the liquid pressure drops below the local saturation pressure. The rapid expansion of vaporized working fluid blocks the flow passages, significantly reducing the hydraulic performance of the equipment. The shock waves generated by collapsing vapor bubbles damage the impeller surface material and ultimately lead to pump failure or malfunction [13]. Additionally, flow-induced vibration and noise from cavitation exacerbate recirculation and vortices within the impeller, causing operational instability and increased energy losses [14]. Under the combined effects of these external working environments and operating conditions, the dynamic characteristics and energy efficiency of the hydraulic system are significantly impacted [15].

The cavitation phenomena and their impacts on pumps differ with various fluid media [16,17]. For instance, heat transfer during cavity growth in room-temperature water is negligible; thus, it is considered as an isothermal fluid. In contrast, the physical properties of thermosensitive fluids such as high-temperature water, Freon refrigerants, and cryogens can change greatly depending on temperature. The temperature drop in the fluid phase transition region leads to a decrease in the saturation pressure, which suppresses the phase transition process. This characteristic is known as the thermal effect [18]. When pumping

low-temperature thermosensitive fluids, the inlet pressure of pumps is often near the saturation pressure. In practical applications, an inducer is often used to improve the flow state within the impeller, thus enhancing the pump performance.

Although high-speed centrifugal pumps using water as a medium have been widely applied, with extensive and in-depth studies on water cavitation, the application of high-speed centrifugal pumps for low-temperature thermosensitive fluids still requires further technical breakthroughs due to differences in thermal properties and pump operating conditions. Research on cavitating flow for refrigerants is also limited. Thus, establishing a deep and comprehensive understanding of the cavitation characteristics and mechanisms of low-temperature thermosensitive fluids is crucial. It is necessary to combine experimental research and numerical simulations to establish a deep and comprehensive understanding of the cavitation characteristics and mechanisms of low-temperature thermosensitive fluids.

This paper reviews the current applications and challenges of high-speed pumps using low-temperature thermosensitive fluids. It proposes a high-speed refrigerant pump solution with hydrodynamic bearings for data center cooling systems, providing guidance for the further development and application of high-speed centrifugal pumps.

2. Applications Status of High-Speed Pumps

2.1. Cryogenic Liquid

Cryogenic pumps often have stringent requirements for weight and volume, and in certain conditions, the flow rate is also very low. Although positive displacement pumps have the advantage of providing a high head at low flow rates, they are complex in structure and less suitable for cryogenic applications. High-speed centrifugal pumps can better adapt to cryogenic working conditions.

Currently, cryogenic pump products are available from only limited global commercial companies, such as Nikkiso (Tokyo, Japan), Cryostar (Hésingue, France), EBARA (Tokyo, Japan), Barber-Nichols (Arvada, CO, USA), etc. These products are primarily designed for large-scale cryogenic systems and come at a high cost [19]. In the realm of basic physics research, cryogenic pumps are commonly employed to transport various cryogenic fluids, including liquid helium, liquid argon, and liquid xenon, as Figure 2 shows. The pumping of these liquid cryogens reduces the temperature to the required experimental cryogenic environment, facilitating the cooling of superconducting coils for applications such as particle detection and control research [20–25]. The applications of cryogenic pumps include the use of liquid helium pumps in CERN's ATLAS Detector, pumping liquid xenon in a gamma-ray detector utilizing liquid Xe as a scintillation material and cooling neutrons using cryogenic fluid circulation systems in the Spallation Neutron Source laboratory, etc.

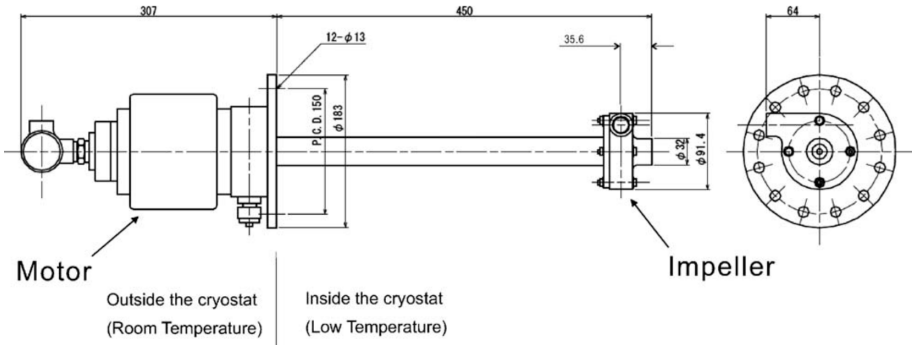

Figure 2. Centrifugal pump with liquid xenon [20].

In industrial production and energy development, the use of liquid cryogens is integral to processes such as air liquefaction and separation, oil well development, and liquefied natural gas (LNG) storage and transportation [26–31]. To facilitate equipment installation, maintenance, and the extraction of cryogens, the pumps employed in these fields are typically submersible pumps, as shown in Figure 3. Moreover, during the design and

selection process of these pumps, it is essential to consider factors such as efficiency, leakage, and reliability to ensure economic and safe operation.

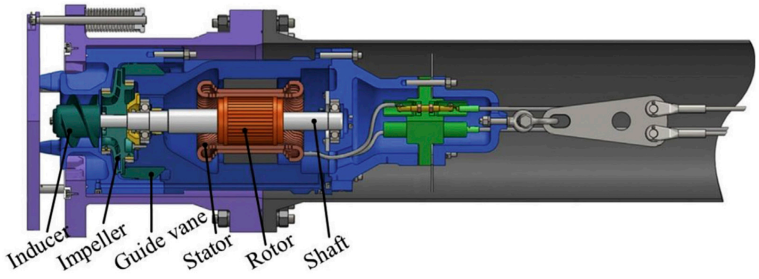

Figure 3. Schematic diagram of LNG submersible pump [26].

Furthermore, cryogenic pumps play a pivotal role in wind-tunnel testing for aerospace applications. Wind tunnels facilitate various aerodynamic experiments based on the principles of relativity and similarity. To increase the Reynolds number within wind tunnels, strategies such as enlarging tunnel dimensions, elevating operating pressure, and reducing the airflow temperature can be employed. Consequently, liquid nitrogen (LN_2) and cryogenic nitrogen are used as simulated flow media in cryogenic wind tunnels, requiring LN_2 pumps that meet high-flow-rate pumping demands [32,33].

The development and promotion of hydrogen energy also necessitate the use of cryogenic pumps for the long-distance transportation and storage of liquid hydrogen (LH_2). These pumps must ensure the continuous and stable delivery of the fluid and handle long-distance, low-flow-rate transportation [34,35]. Another significant application of high-speed cryogenic pumps is within the aerospace industry [36–39]. Modern liquid rocket engines are advancing toward a high specific impulse and environmental sustainability, typically utilizing cryogenic propellants such as LH_2 and liquid oxygen (LOX). Turbopumps are employed to supply these cryogenic propellants to combustion chambers operating under extremely high pressure. Unlike closed-loop cryogenic systems, turbopumps are characterized by high flow rates and very high rotational speeds, as illustrated in Figure 4. The design of the impeller profile, internal flow-field distribution, rotor stress distribution, and pump performance are critical factors in these applications.

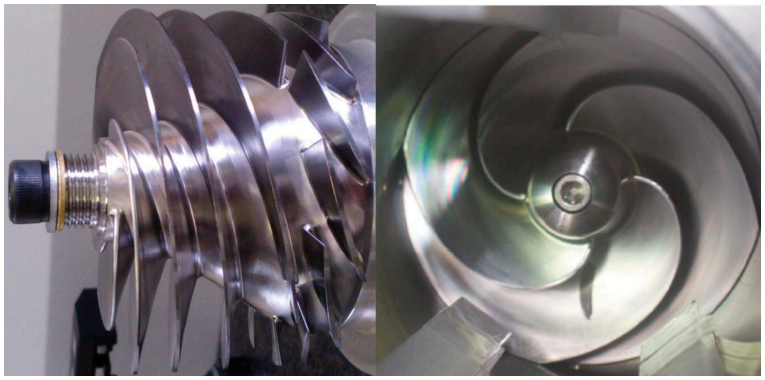

Figure 4. Liquid rocket engine turbopump with inducer [40].

2.2. Liquid Refrigerant

The procurement and storage of liquid cryogenic fluids are challenging and expensive, making the setup and operation of cryogenic test rigs costly and experimentally demanding. As illustrated in Table 1, the physical properties of refrigerants closely resemble those of cryogens. There are substantial differences between the physical properties of room-temperature water and cryogens, particularly concerning the saturation pressure change with the temperature increase dp_v/dT, liquid/vapor density ratio ρ_l/ρ_v, latent heat of

vaporization c_p, thermal conductivity k, and viscosity ν. Consequently, some researchers use R114 refrigerant as a surrogate for cryogens, applying similarity laws to investigate the internal flow and hydraulic performance of refrigerants in centrifugal pumps [18].

Table 1. Thermal properties of thermosensitive fluids vs. room-temperature water.

Parameters	Water	LN_2	LH_2	R114	R134a	R410A
T/K	283	77	23	283	283	283
dp_v/d_T/Pa·K^{-1}	84	12,108	53,690	4700	13,980	32,500
ρ_l/ρ_v	107,286.1	182.0	26.7	154.0	62.7	27.5
c_p/kj·kg^{-1}	2477.5	199.6	431.2	133.7	190.9	/
k/mW·m^{-1}·K^{-1}	578.4	145.5	103.4	64.3	87.7	97.5
ν/μPa·s	1311.7	162.9	11.0	325.8	235.3	143.0

With the rapid advancement of electronic information technology and increased focus on energy conservation, devices are becoming smaller and more powerful, leading to higher heat fluxes [41]. Pump-driven two-phase flow systems have been increasingly utilized for cooling high-heat-flux electronic devices and data centers due to their superior heat transfer capabilities and energy efficiency. The primary working fluids in these systems include fluorocarbons such as R142b, R22, R32, and R410A [42–45]. Our research team has previously developed a high-speed pump utilizing R134a refrigerant [46]. This single-stage pipeline pump is suitable for high-heat-flux electronic thermal management systems, which is shown in Figure 5. During operation, the refrigerant upstream of the pump is in a low-temperature and low-pressure state. After being pressurized by the refrigerant pump, it enters the cooling equipment. The net positive suction head (NPSH) is a critical factor influencing the pump performance.

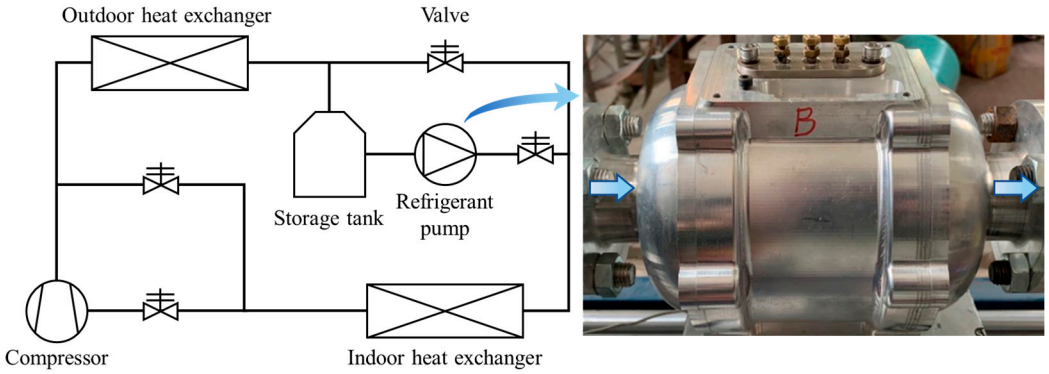

Figure 5. Pump-driven two-phase cooling loop using high-speed R134a refrigerant pump.

3. Current Challenges

3.1. Cavitation in Inducer

Cavitation generally occurs at the inlet of centrifugal pumps and is more likely to occur at high rotational speeds [47]. Cavitation not only damages the blade material, thereby reducing the operational lifespan of pumps, but also induces pressure pulsations that lead to vibrations. These vibrations can jeopardize the safe and stable operation of aerospace engines or petrochemical systems or cryogenic systems. Additionally, high-frequency noise (above 500 Hz) and a reduction in pump capacity are observed. In rocket engines, high-speed turbopumps are subject to size constraints, with impellers rotating at extremely high speeds, resulting in severe cavitation of the propellant. Numerous rocket launch failures have been attributed to the instability caused by turbopump cavitation. In industrial systems, cavitation in cryogenic fluids not only reduces production line efficiency but also impacts the resonance of transport pipelines.

For high-speed centrifugal pumps, radial impellers offer significant pressure-boosting capabilities but are highly sensitive to cavitation, making them susceptible to breakdown.

Presetting an axial-flow inducer is an effective solution to the cavitation problem. While the pressure-boosting capability of an inducer is lower than that of a radial impeller, it provides superior cavitation resistance. Extensive studies have been conducted on the cavitation behavior of low-temperature thermosensitive fluids within inducers, primarily using safe and readily available LN_2.

Ito et al. [48] introduced a bubble size distribution model into numerical simulations to investigate the cavitation characteristics of LN_2, focusing on bubble development and thermal effects. Numerical results indicated that the rotational speed of the backflow vortex is consistently lower than that of the impeller and is concentrated near the inducer axis, with bubbles of different sizes exhibiting relatively fixed positional distributions. Chen et al. [49] examined the mechanism of tip leakage vortex cavitation and the associated cavity structure in inducers. Their numerical results demonstrated that the periodic coupling of cavity development, flow rate, and local incidence angle variations led to the instability of tip leakage vortex cavitation. The axial vorticity distribution of the tip leakage vortex and the cavity structure are shown in Figure 6. Zhang et al. [50] evaluated the prediction accuracy of four cavitation models—full cavitation, Kunz, Schnerr–Sauer, and Zwart–Gerber–Belamri models—using Ito et al.'s [51] experimentally captured images of LN_2 cavitation as a reference. The full cavitation model provided the most accurate numerical predictions without modifying computational parameters, whereas the other models achieved satisfactory predictions through empirical parameter adjustments. This demonstrates that by improving computational models and validating them against experimental results, CFD numerical simulations can achieve high computational accuracy, providing reliable guidance for analyzing hydrodynamic phenomena in hydraulic devices [52].

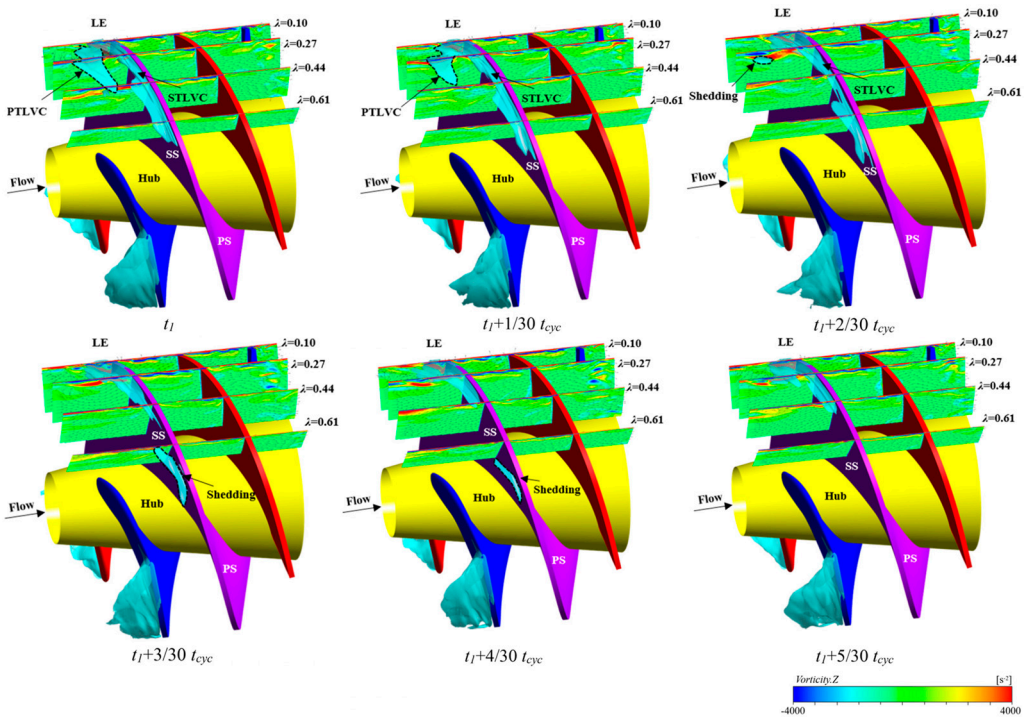

Figure 6. Axial vorticity distribution and cavity evolution of tip leakage vortex in inducer [49].

In addition to LN_2, cavitation in cryogenic propellants such as LH_2 and LOX used in liquid rockets has also received considerable attention and research. In an experimental study, Lettieri et al. [40] conducted visual studies on the cavitation instability of the inducer in rocket engine turbopumps. Optical experiments demonstrated that the generation of rotating cavitation is related to the interaction between cavities at the leading edges of adjacent blades. Changes in the incidence angle exacerbate cavitation, leading to the apparent supersynchronous rotation of the cavities around the annulus. Shao and Zhao [34,53]

developed a LH_2 centrifugal pump to meet the demand for low-flow-rate and high-head applications. They conducted hydraulic performance tests on a prototype designed using LN_2 as the working fluid, employing similarity laws. The pump performance met the design expectations, with simulation results closely matching experimental data. Based on this, they optimized the impeller design using genetic algorithms. Cavitation characteristics can be effectively enhanced by decreasing the inlet angle, enlarging the impeller diameter, or incorporating an inducer. Additionally, slightly reducing the impeller's outlet diameter can decrease hydraulic losses, thereby increasing the head. The performance characteristics are shown in Figure 7. Kim et al. [54,55] used water at 310–323 K and LOX as working fluids to study cavitation instability by measuring the vibration of the pump casing. Under low-flow-rate conditions, both fluids exhibited supersynchronous rotating cavitation. In the LOX experiments, asymmetric cavitation was predominant, and its cavitation instability at high-flow-rate conditions was lower than that of hot water. Shimura et al. [56] conducted experimental studies on the vibrations caused by cavitation in the inducer of a turbopump and modified the inducer blades to suppress rotating cavitation and mitigate vibration effects.

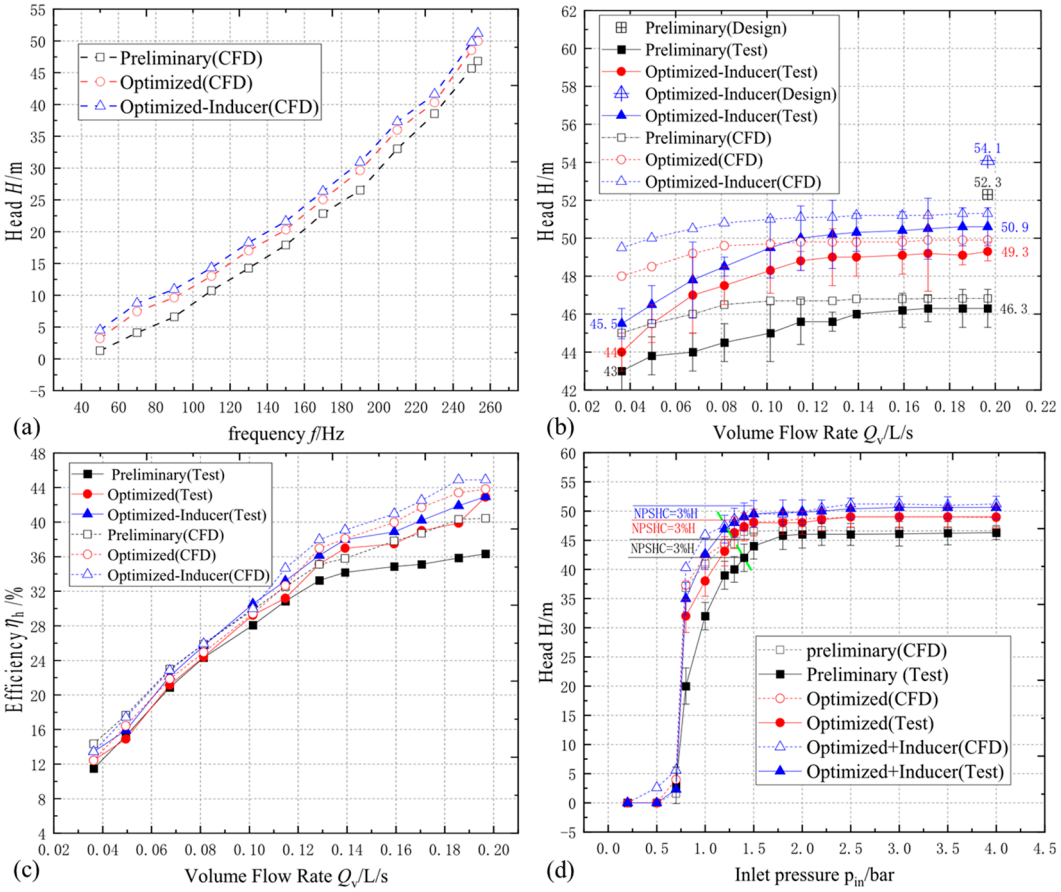

Figure 7. Effect of the inducer on the hydraulic and cavitation performance of the LH_2 pump: (**a**) frequency–head curve, (**b**) flow rate–head curve, (**c**) flow rate–efficiency curve, and (**d**) NPSH–head curve [34].

Tani et al. [11] studied the relationship between rotating cavitation and the flow coefficient in the oxidizer inducer of a turbopump. Numerical simulations discussed the relationship between tip vortices and inducer blades, while unsteady simulations revealed that tip vortices were not the primary factor driving cavitation. Instead, negative flow divergence caused by bubble collapse affected the flow angle, leading to tip gap recirculation and exacerbating cavitation. Kimura et al. [57] investigated the tip leakage vortex structure and the rotating cavitation it induced. Their study found that the development of

the vortex structure is strongly influenced by the geometry of the inlet casing and flow rate. Adding a gutter to the inlet casing effectively suppressed cavitation and recirculation, as shown in Figure 8.

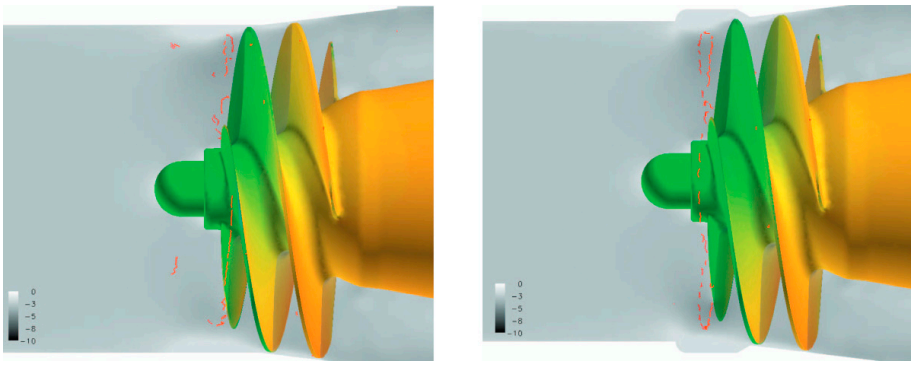

Figure 8. Suppression of backflow cavitation in the inducer by gutter at the inlet casing [57]. The distribution of the axial velocity component is plotted on the plane, which includes the rotation axis by a gray-scale contour map. The brightest area represents the backflow region. Red lines and the colored inducer indicate the vortex cores and pressure, respectively.

Research on cavitation in inducers for LNG has also been extensive. Son et al. [28] developed a pump for LNG transportation systems, investigating its hydraulic performance and NPSH and addressing cavitation and surge issues. Their study revealed that the pressure loss generated within the inducer is not recovered in the impeller and recirculation channels, and this pressure loss further increases. Vortices generated at the trailing edge of the blades negatively affect the operation of the impeller and the hydraulic performance of the pump. Li et al. [27] performed both numerical and experimental studies on the cavitation behavior and pressure pulsation of the impeller in a two-stage LNG submersible pump. Their research found that as the flow rate increases, cavitation becomes more severe and periodic, with a greater impact on the first-stage impeller. The low-frequency pressure pulsation frequency of the impeller gradually becomes dominant. Karakas et al. [58] also performed numerical and experimental studies on the effects of inducer tip clearance on the cavitation characteristics and hydraulic performance of an LNG submersible pump. The results indicated that wider inducer tip clearances lead to back leakage and more severe vortex recirculation, resulting in local pressure drops and cavitation. Moreover, the impact of tip clearance on cavitation is more pronounced in variable pitch inducers.

3.2. Thermal Effect

The temperature reduction induced by thermal effects is a characteristic of cavitation in thermosensitive fluids, which complicates the cavitation behavior and has been a significant area of research in low-temperature thermosensitive fluid cavitation studies. Thermal cavitation not only suppresses the formation and growth of cavities but also impacts the cavitation dynamics of thermosensitive fluids [59,60].

Researchers have extensively studied the cavitation dynamics in simple cavity-generating devices such as hydrofoils, Venturi tubes, and ogives [61–63]. Chen et al. [64] developed a hydrofoil cavitating flow model using fluoroketone as the working fluid and discovered that the thermodynamic cavitation effects of room-temperature fluoroketone resemble those of LN_2 at cryogenic temperatures. Their findings identified a transition temperature at which the dominant factor influencing cavitation shifts from the liquid/vapor density ratio to thermal effects. Zhang et al. [65] carried out experimental studies on the cavitation characteristics of R134a refrigerant in a Venturi tube and observed that the formation, shedding, and collapse of cavities become more frequent and complex under the combined influence of reentrant jet flow and thermal effects.

For cryogens, Chen et al. [66] examined the influence of thermal effects on the cavitating flow of LN_2 in a hydrofoil, discussing how thermal effects specifically impact the mass transfer processes and cavity structures in cavitating flows. They found that the phase transition of cryogenic liquids causes changes in fluid properties, which in turn alter the reference free-stream conditions equivalently. Long et al. [67] performed numerical studies on the shedding process of LH_2 cavitation on an ogive surface under thermal effects, clarifying the interaction between cavitation and vortices in unsteady thermal cavitating flows. Chen et al. [68,69] investigated the thermal transition process and transition temperature in the evolution of unsteady cavitating flows of LN_2, identifying two modes of thermal cavitation dynamics, termed the inertial mode and thermal mode, as shown in Figure 9. As the temperature rises, the shedding frequency and the number of simultaneously shedding cavities increase consistently, while the characteristic frequency of individual shedding processes and quasi-periodic features first decreases and then increases. Zhu et al. [70,71] visualized the cavitating flow of LN_2 in a Venturi tube and established a one-dimensional theoretical equation considering thermal effects to estimate the speed of the condensation front, applying a two-dimensional thermal effect parameter to quantify the intensity of cavitation thermal effects. Murakami and Harada [72] utilized Particle Image Velocimetry to investigate the cavitating flow of superfluid helium, focusing on the effect of the void fraction in the Venturi tube on cavitation thermal effects. Niiyama et al. [73] studied the influence of turbulence around cavities on cavitation thermal effects based on LN_2 cavitation experiments in an orifice, finding that heat transfer is enhanced during cavitation. Liang et al. [74] demonstrated that the thermal cavitation mode transition of LH_2 is influenced by both thermal effects and Reynolds number, with the entropy production rate increasing with temperature according to the entropy transport equation.

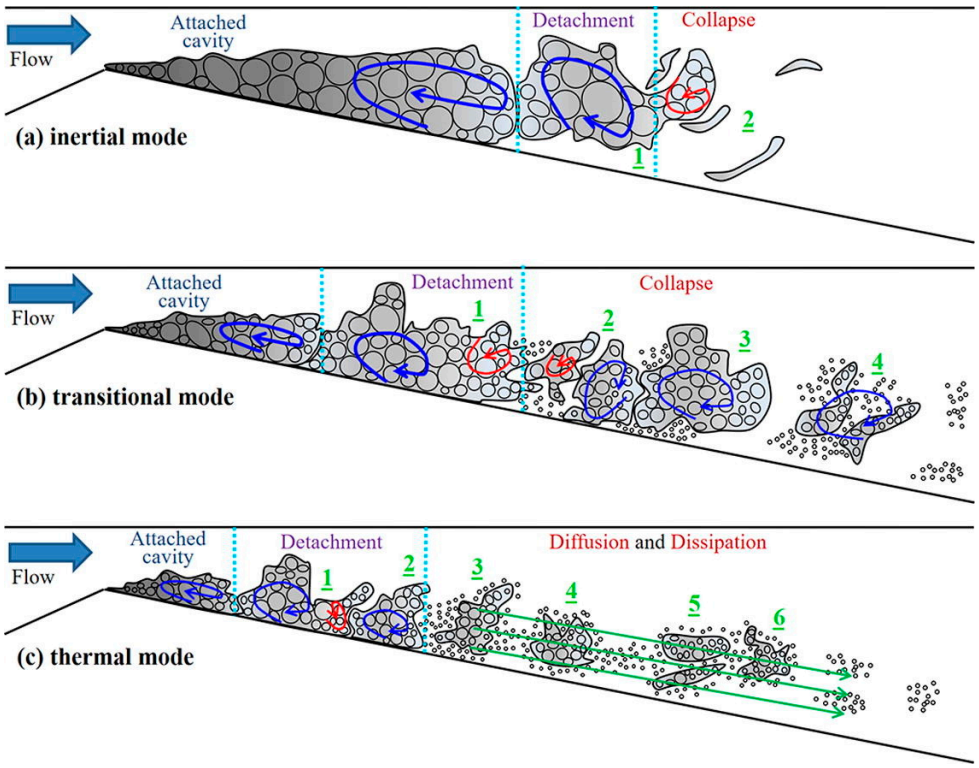

Figure 9. Cavity shedding of LN_2 cavitation under different thermal cavitation modes. Within the gray-shaded cavities, the curves with blue and red arrows represent the direction of cavity rotation. The green straight line with arrows represents the movement of the detached cavity. The numbers indicate the cavity shedding process [69].

As a complex three-dimensional hydraulic structure, the study of cavitation behavior within an inducer holds significant practical value. Extensive research on the thermal effects of cavitation within inducers has been conducted through a combination of experimental and simulation approaches. Yoshida et al. [75–77] studied the thermal effects of LN_2 on synchronous rotating cavitation within an inducer, examining characteristics such as the cavity length at the blade tip, temperature, and fluid forces. They found that, as the cavity length increased, the thermal effects intensified. The growth of cavity non-uniformity due to synchronous rotating cavitation was identified as a primary cause of shaft vibration. Ito et al. [51,78] established the first visualization experimental setup suitable for studying an inducer with both LN_2 and water, comparing the unsteady cavitation characteristics of LN_2 to those of water, as shown in Figure 10. They elucidated the cavitation developments of backflow vortices and tip vortices as well as the thermal effects of cryogen. The experimental results indicated that backflow vortices in LN_2 cavitation are more intense, and tip vortices are smaller compared to those in water.

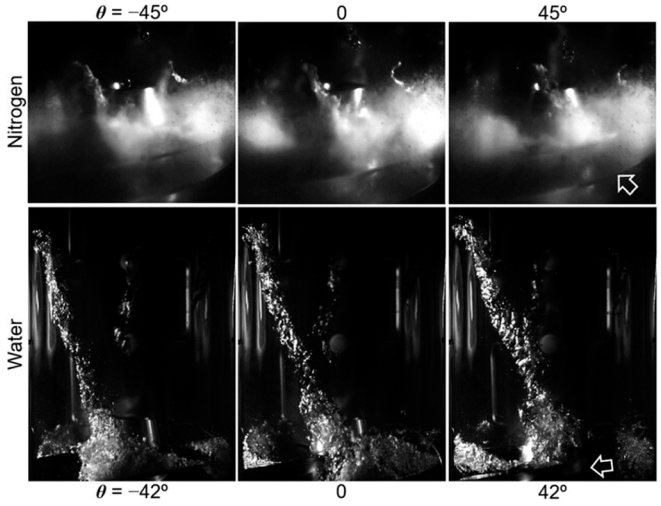

Figure 10. Tip vortex and backflow vortex cavitation occurring on the inducer with thermosensitive fluid LN_2 vs. room-temperature water. The arrows indicate the locations where tip vortex and backflow vortex occur [48].

Building on this visualization experiment, Fan et al. [79] set a cavitation model to predict the performance of the LN_2 inducer. Their numerical study revealed that, in the cavitation region, as temperature increased, the temperature drop within the cavities became significant and the cavity volume decreased, contributing to a delay in the head variation. Additionally, an increased rotational speed affected the cavity volume, exacerbating cavitation. They also analyzed sub-synchronous rotating cavitation phenomena in an inducer in terms of a temperature drop, thermal effects, and bubble volume changes. Chen et al. [80] utilized an enhanced cavitation model that includes thermal effects to investigate how cavitation and tip leakage vortices influence hydraulic losses in an LN_2 inducer. They found that the tip leakage flow exhibited a helical distribution, with its shape negatively correlated with the nitrogen temperature. Thermal effects partially suppressed the development of tip leakage vortices. Enstrophy analysis revealed energy losses within tip leakage vortices, identifying these vortices as key parameters influencing thermal cavitation. Wei et al. [81] investigated cavitating flow characteristics in a LN_2 submersible pump. They improved the cavitation model by incorporating corrections for rotation and thermal effects and validated their numerical framework by comparing it with transient cavitation images captured by Ito et al. [51]. Their study indicated that cavitation within the inducer was primarily caused by vortices at the tip clearance, with the evolution of cavities shown in Figure 11. Using vortex identification methods and the vorticity transport equation, they

identified vortex structures, analyzed the interaction between cavitation and vortices, and assessed the impact of thermal effects on cavitation.

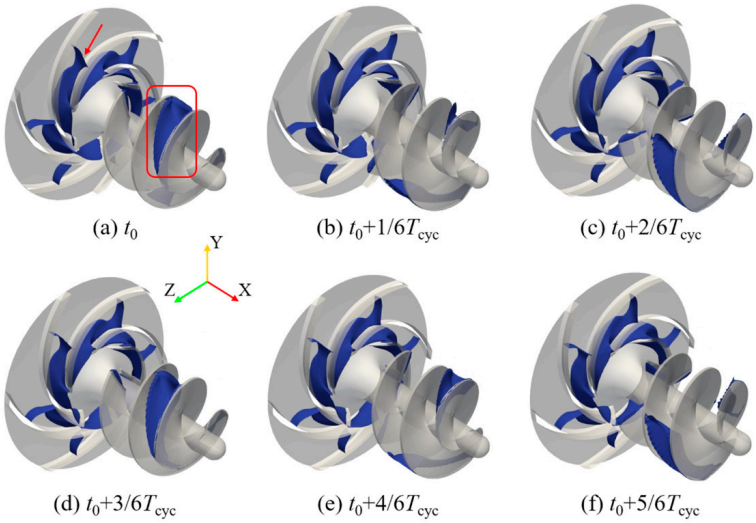

Figure 11. The cavity evolution of LN_2 cavitation, considering thermal effects [81].

Blumenthal and Kelecy [82] incorporated the thermal properties of LH_2 into a cavitation model and utilized CFD methods to predict the cavitating flow state of the NASA TM X-1360 inducer with LH_2. The revised numerical model provided the most accurate predictions at 23.3 K. Goncalves et al. [83] conducted numerical investigations into the cavitating flow characteristics of LH_2 and LOX within the inducer of a NASA rocket engine turbopump. Their computational model accounted for the impact of the thermal properties of cryogens on the flow characteristics, revealing that, at high rotational speeds, the wall viscosity effect and vaporization, respectively, led to heating and cooling effects within the pump.

Xiang et al. [37,84] analyzed the internal cavitating flow characteristics of an inducer using LOX as the working fluid based on a transport-based cryogen cavitation model. Their findings indicated that thermal effects significantly reduced the cavitation region and bubble formation, thereby delaying the head breakdown, as illustrated in Figure 12. Higher temperatures exhibited stronger thermal effects and improved cavitation performance. Shi et al. [85] explored the thermal cavitation characteristics of LOX, discovering that, as the temperature was raised, the thermal effects became more pronounced, effectively suppressing cavitation phenomena in steady-state cavitating flows within the inducer.

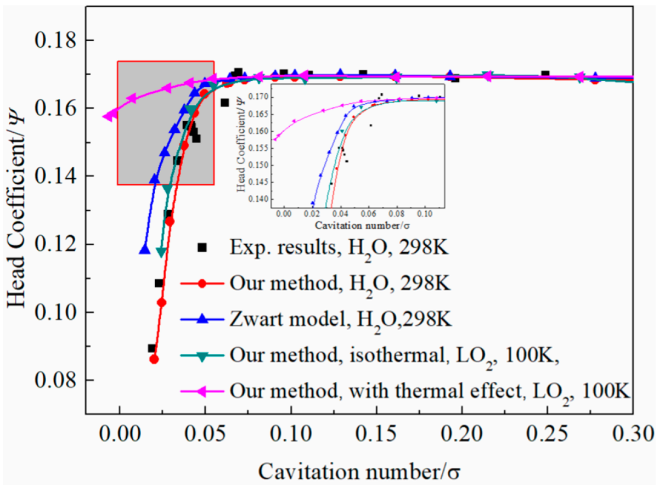

Figure 12. The impact of the thermal effect on the hydraulic performance of pump [84].

As more commonly used thermosensitive fluids, refrigerants have practical significance for engineering applications in the study of their cavitation thermal properties. Holl et al. [86] developed a correlation for temperature depression based on temperature and pressure from cavitation experiments with water and Freon R113 to describe cavitation intensity. Franc et al. [18,87] performed visualization experiments on the cavitating flow of R114 refrigerant within an inducer, exploring how temperature affects cavitation development, as shown in Figure 13. They estimated the temperature drop around the cavitation region based on the cavity length, finding that the temperature drop increased with an increasing cavity length. Additionally, they established a model for analyzing the thermal effects of cavitation in inducers. Fang et al. [46] employed an improved Sauer–Schnerr cavitation model to investigate the impact of variables such as NPSH, temperature, and flow rate on the internal flow characteristics and cavitating flow properties of a centrifugal pump with an inducer.

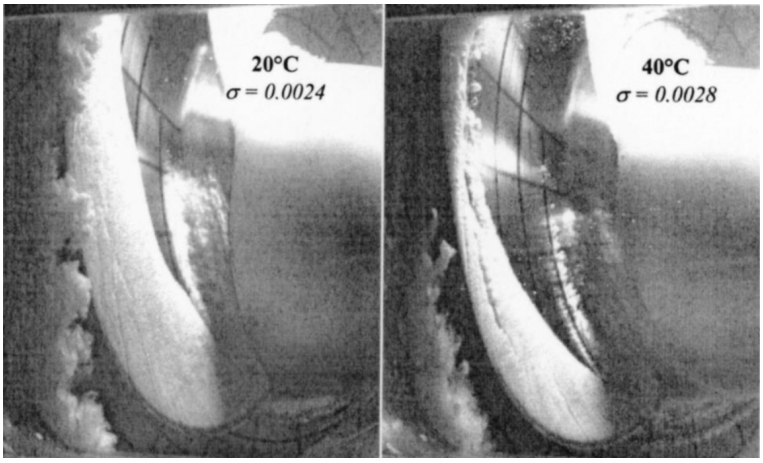

Figure 13. The impact of temperature on the R114 refrigerant cavitation [18].

The cavitating flow of low-temperature thermosensitive fluids within the inducer is highly unsteady, with its evolution process accompanied by dramatic changes in physical quantities such as temperature, pressure, and velocity. Due to the suppression of thermal effects, the interaction mechanism between the cavitating flow and turbulence, as well as vortex structures in the flow field, becomes more complex. Therefore, conducting experimental studies on cavitation in the inducer with low-temperature thermosensitive fluids is valuable for revealing the mechanisms of cavitating flow.

The importance of synchronously collecting multiple physical parameters, such as pressure, temperature, and frequency, and using high-speed photography and Particle Image Velocimetry (PIV) technology to study cavitating flow is increasing. However, when the working fluid temperature is below room temperature, especially for cryogenic fluids, setting up cavitation visualization testing equipment is highly challenging due to limitations in adiabatic conditions, frosting on visual windows, material brittleness, and high-speed rotating mechanical processing techniques.

Numerical simulation has become an indispensable research method for solving complex multiphase cavitating flow problems. Extensive and in-depth research on the calibration and improvement of cavitation models and turbulence models can accurately present and predict the cavitating flow of low-temperature thermosensitive fluids within the inducer. Additionally, the suppression of cavity evolution by thermal effects has also received attention. Furthermore, the use of data-driven methods to perform the modal decomposition of cavitating flow and obtain coherent structures of cavitating flow is also worthy of attention.

4. Prospects and Solutions

4.1. Development of a Low-Specific-Speed Centrifugal Pump with an Inducer

In large systems, high-flow-rate cryogenic pumps have been successfully implemented. However, for small systems, due to factors such as the flow resistance of the pipeline and components, pumps need to have characteristics that can handle low flow rates and high pumping pressures, which is indicative of a lower specific speed. Based on the summary of current applications and challenges, the development of low-specific-speed pumps with high performance metrics will be the future trend and direction for centrifugal pumps utilizing thermosensitive fluids.

The development of low-specific-speed pumps will focus on the following directions:

1. Enhancing cavitation resistance: Incorporating an inducer at the pump inlet to enhance the NPSH, thereby mitigating the effects of high rotational speeds and complex operating conditions on pump performance. The design of the inducer should account for the impacts of cavitation dynamics and thermal effects.
2. Optimizing impeller design: optimizing impeller profile design methods to improve hydraulic performance, addressing issues of high energy loss and low efficiency at ultra-low specific speeds.
3. Flow-induced noise and vibrations: attention should be given to flow-induced noise and bearing vibrations during high-speed operation, as the performance of high-speed bearings directly influences the operational lifespan of the pump.
4. Compact and maintenance-friendly design: the pump design should be more compact and easier to maintain, with efforts to reduce the weight and volume while also lowering manufacturing and operational maintenance costs.

4.2. Application of a Centrifugal Pump with Hydrodynamic Bearings

4.2.1. The Structural Design of the Prototype

Building on the previous applications review, naturally cooled pump-driven two-phase flow systems have significant development potential for data center cooling. Considering the actual working conditions of vapor-compression refrigeration systems, we propose a high-speed centrifugal pump with hydrodynamic bearings, utilizing R410A refrigerant as the working fluid. The design operating conditions are a flow rate of 1.5 m^3/h and a designed rotational speed of 7000 rpm. To ensure hydraulic efficiency, a two-stage impeller configuration is employed, with specific speeds of $n_{q1} = 15$ and $n_{q2} = 11$ for each stage, respectively. The primary components of the high-speed centrifugal pump, as shown in Figure 14, include the inducer, primary impeller and vaned diffuser, secondary impeller and vaned diffuser, discharge volute, hydrodynamic bearing, shaft, motor, and casing. Considering the weight and strength of the prototype, the pump casing, vaned diffuser, and discharge volute are made of aluminum alloy, while the shaft, impeller, hydrodynamic bearings, and bearing housing are made of stainless steel.

To achieve the high-speed rotation of the pump, herringbone-grooved radial hydrodynamic bearings and spiral-grooved thrust hydrodynamic bearings are employed as support components, using R410A refrigerant as the lubricating medium. The hydrodynamic effect of the liquid maintains the high-speed operation of the motor. Since the bearing rotating surface does not come into direct contact with the bearing housing, the friction loss and wear of the hydrodynamic bearings are minimal, resulting in smooth operation, high reliability, and low noise [88].

To further integrate the pump structure, the motor is housed within the casing, eliminating the need for couplings and other transmission components. The high-speed centrifugal pump is designed for a pipeline configuration. The working fluid is initially drawn in from the inlet to the inducer for pre-pressurization; then it enters the primary impeller and vaned diffuser, flows through the motor casing to the secondary impeller and vaned diffuser, and is finally discharged through the volute. The design parameters of the hydraulic components are listed in Table 2.

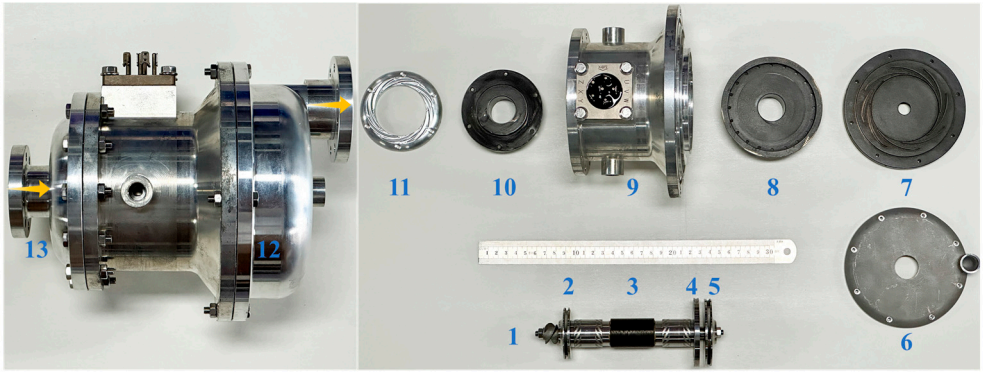

1 – Inducer, 2 – Primary impeller, 3 – Shaft with radial hydrodynamic bearing and magnetic steel, 4 – Thrust hydrodynamic bearing, 5 – Secondary impeller, 6 – Discharge volute, 7 – Secondary vaned diffuser, 8 –Secondary bearing housing, 9 – Motor casing, 10 – Primary bearing housing, 11 – Primary vaned diffuser, 12 – Posterior casing, 13 – Anterior casing

Figure 14. Major components of two-stage centrifugal refrigerant pump. The arrows indicate the direction of fluid flow.

Table 2. Main parameters of hydraulic components.

Design Parameter		Value
Inducer	Number of blades	3
	Inducer diameter/mm	21.4
	Hub diameter/mm	12
	Tip clearance/mm	0.3
Primary impeller	Number of blades	6
	Inlet diameter/mm	22
	Outlet blade angle/°	28
	Outlet width/mm	3
	Outlet diameter/mm	52
Primary vaned diffuser	Number of blades	8
	Outlet blade angle/°	12
	Outlet diameter/mm	68
Secondary impeller	Number of blades	6
	Inlet diameter/mm	19
	Outlet blade angle/°	30
	Outlet width/mm	3
	Outlet diameter/mm	68
Secondary vaned diffuser	Number of blades	8
	Outlet blade angle/°	12
	Outlet diameter/mm	88
Discharge volute	Inlet width/mm	3.6
	Discharge diameter/mm	18

4.2.2. Research Methods

As previously reviewed, CFD numerical calculations can shorten the design time and reduce manufacturing costs for the development of new pump models. The development process of the centrifugal pump with a hydrodynamic bearing combined with CFD numerical performance predictions and experimental testing for validation. First, the profiles of the main hydraulic components, such as the impeller, were designed. Suitable numerical models were selected to predict the pump performance. Subsequently, tests were conducted on a refrigerant pump external characteristic test rig, with experimental results guiding the pump design and numerical simulation outcomes.

Pressure and temperature measurement points were placed at both the inlet and outlet of the prototype. A flow meter and flow valve were installed downstream of the pump, while the inflow pressure at the pump upstream could be adjusted by changing the height

of the refrigerant storage tank. The refrigerant pump test rig allowed the determination of key parameters such as the head and power under different flow rates, speeds, and NPSH conditions. These parameters were recorded using a data acquisition system to infer the operating status of the pump. Additionally, an automatic control system enabled start/stop testing and long-term operational testing of the prototype.

4.2.3. Test Results of Prototype

Tests were conducted on the constructed refrigerant pump external characteristic test rig. The prototype had an inlet temperature of 10 °C and an NPSH of 3 m. The hydraulic performance test results of the high-speed centrifugal pump at the rated speed are shown in Figure 15. Under the design conditions, the pump achieves a head of 56.5 m with an efficiency of 36.1%. It can be observed that, when the prototype operates at the rated speed, the head gradually decreases with the increasing flow rate, without exhibiting a hump. The power increases at a relatively gentle rate with the increasing flow rate. The flow rate–efficiency curve reaches a peak and then decreases as the flow rate increases, indicating an optimal flow rate at which the prototype achieves maximum efficiency. The maximum efficiency point (BEP) of the centrifugal pump at the rated speed is 37.9%, with a corresponding flow rate of 2.1 m^3/h and a head of 47.5 m. The trend of the hydraulic characteristics of the prototype obtained from the experiments was consistent with the hydraulic characteristics of pumps with similar specific speeds studied in Ref. [89]. The process of pumping liquid refrigerant was continuous and stable, meeting design expectations. Compared to an earlier single-stage high-speed centrifugal pump developed by the research team that used water as the working fluid, the prototype achieved higher efficiency at a lower designed specific speed [12].

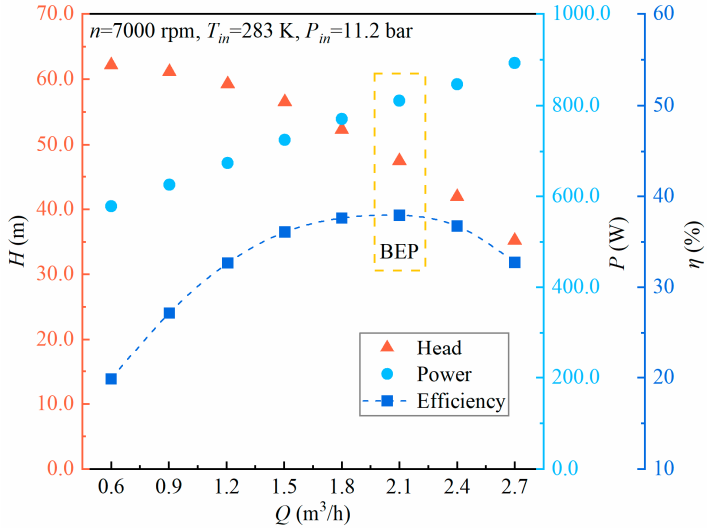

Figure 15. Experimentally obtained external characteristic curve of the prototype.

The designed high-speed pump can adapt to a broader range of applications through variable frequency motor control. According to similarity laws, pumps operating under approximately similar conditions exhibit nearly equal efficiencies. Using the BEP at the design speed as a baseline, predictions for similar conditions at speeds ranging from 4000 to 6000 rpm were made and compared with measured data, as shown in Figure 16. The experimentally measured efficiencies at 4000 rpm, 5000 rpm, and 6000 rpm were 36.7%, 37.8%, and 37.4%, respectively. It can be seen that the deviation between the theoretical predictions and the experimental results for the head and power increases as the rotational speed decreases, with a maximum deviation of 2.4%. This demonstrates that similarity laws provide accurate predictions of the hydraulic performance of centrifugal pumps under various operating conditions.

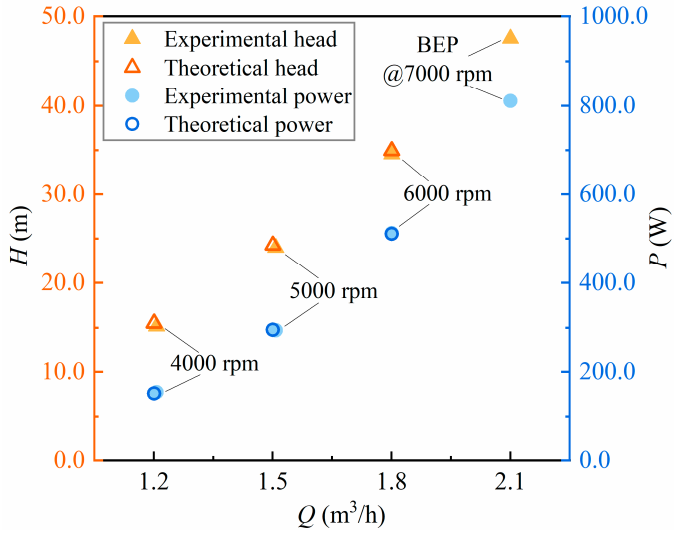

Figure 16. The theoretical and experimental values of the BEP at different rotational speeds.

Additionally, the reliability and service life of the hydrodynamic bearings in the centrifugal pump were empirically evaluated. The pump successfully underwent over 100,000 on/off cycles and more than 150 days of continuous overload operation testing within a data center cooling system. After the tests, the degradation in the external characteristics of the high-speed centrifugal pump was less than 5%. This prototype demonstrates substantial application potential in data center cooling systems and novel electronic device cooling technologies.

5. Conclusions

This paper summarizes the current applications of high-speed pumps using low-temperature thermosensitive fluids and reviews the challenges encountered in their application. These challenges include the mechanisms of cavitation inception, development, and collapse within the inducer as well as the impact of fluid thermal properties and thermal effects on cavitating flow. Understanding these aspects is crucial for studying the performance of high-speed pumps and guiding their design. Based on industry development trends, a high-speed centrifugal refrigerant pump incorporating hydrodynamic bearings is proposed, with an overview of its performance and potential applications. The key conclusions drawn from this review and discussion are as follows:

(1) Cavitation is the most common issue encountered in the pumping process of high-speed pumps. An inducer can enhance the cavitation resistance of pumps, significantly improving their hydraulic performance and stability. The accurate prediction of the cavitation intensity in an inducer using improved cavitation models is crucial for the effective design and performance optimization of high-speed pumps.

(2) Compared to cavitation studies with room-temperature water, cavitation experiments with low-temperature thermosensitive fluids are relatively few due to the complexity and difficulty of setting up the testing systems. Capturing cavity flow behavior through high-speed photography has become one of the important research methods for exploring cavitation characteristics and mechanisms. However, limited by current technological conditions, conducting cryogenic cavitation flow experiments in inducers is extremely challenging.

(3) Thermal effects have become the focus of research on cavitation dynamics of thermosensitive fluids. The local temperature drop caused by thermal effects suppresses the growth and collapse of cavities. Affected by the thermal effects, the cavitating flow characteristics in hydraulic components such as hydrofoils, Venturi tubes, and inducers have been extensively studied and demonstrated.

(4) A two-stage high-speed refrigerant pump with an inducer and hydrodynamic bearings is proposed. Under design conditions (n = 7000 rpm, Q = 1.5 m^3/h), the pump achieves a head of 56.5 m with an efficiency of 36.1%. The stability and reliability of the prototype have been thoroughly validated, indicating significant application potential in data center cooling systems and novel electronic device cooling technologies.

Author Contributions: Writing—original draft preparation, B.Z.; investigation, B.Z. and B.N.; data curation, B.N.; validation, Z.Z.; formal analysis, B.Z. and Z.Z.; writing—review and editing, S.C. and Y.H.; resources, S.C.; funding acquisition, R.X.; supervision, Y.H. All authors have read and agreed to the published version of the manuscript.

Funding: This research was funded by the National Natural Science Foundation of China (Project No. 52276017) and the Youth Innovation Team of Shaanxi Universities.

Conflicts of Interest: The authors declare no conflicts of interest.

References

1. Lobanoff, V.S.; Ross, R. *Centrifugal Pumps: Design and Application*; Elsevier: Amsterdam, The Netherlands, 1985.
2. Shah, S.R.; Jain, S.V.; Patel, R.N.; Lakhera, V.J. CFD for Centrifugal Pumps: A Review of the State-of-the-Art. *Procedia Eng.* **2013**, *51*, 715–720. [CrossRef]
3. Stosiak, M.; Karpenko, M.; Prentkovskis, O.; Deptuła, A.; Skačkauskas, P. Research of Vibrations Effect on Hydraulic Valves in Military Vehicles. *Def. Technol.* **2023**, *30*, 111–125. [CrossRef]
4. Choi, J.H.; Kim, N.-H.; Kogiso, N. Reliability for Aerospace Systems: Methods and Applications. *Adv. Mech. Eng.* **2016**, *8*, 168781401667709. [CrossRef]
5. Gülich, J.F. *Centrifugal Pumps*; Springer International Publishing: Cham, Switzerland, 2020; ISBN 978-3-030-14787-7.
6. Li, W.; Yang, Q.; Yang, Y.; Ji, L.; Shi, W.; Agarwal, R. Optimization of Pump Transient Energy Characteristics Based on Response Surface Optimization Model and Computational Fluid Dynamics. *Appl. Energy* **2024**, *362*, 123038. [CrossRef]
7. Li, Y.; Liu, D.; Cui, B.; Lin, Z.; Zheng, Y.; Ishnazarov, O. Studying Particle Transport Characteristics in Centrifugal Pumps under External Vibration Using CFD-DEM Simulation. *Ocean Eng.* **2024**, *301*, 117538. [CrossRef]
8. Rorro, F.; Fiusco, F.; Broman, L.M.; Prahl Wittberg, L. Backflow at the Inlet of Centrifugal Blood Pumps Enhanced by Geometrical Features. *Phys. Fluids* **2024**, *36*, 037127. [CrossRef]
9. Zhang, Y.-L.; Li, W. A Precisive Calculation Method of Volumetric and Hydraulic Efficiency of Centrifugal Pumps. *Phys. Fluids* **2023**, *35*, 077104. [CrossRef]
10. Lin, X.; Zhang, B.; Zhang, M.; Zhao, Y.; Lai, T.; Chen, L.; Xue, R. Influence of Internal Flow on the Performance of High-Speed Centrifugal Pumps with a Fully Sealed Structure. *Appl. Sci.* **2022**, *12*, 5263. [CrossRef]
11. Tani, N.; Yamanishi, N.; Tsujimoto, Y. Influence of Flow Coefficient and Flow Structure on Rotational Cavitation in Inducer. *J. Fluids Eng.* **2012**, *134*, 021302. [CrossRef]
12. Xue, R.; Lin, X.; Zhang, B.; Zhou, H.; Lai, T.; Hou, Y. CFD and Energy Loss Model Analysis of High-Speed Centrifugal Pump with Low Specific Speed. *Appl. Sci.* **2022**, *12*, 7435. [CrossRef]
13. Čdina, M. Detection of cavitation phenomenon in a centrifugal pump using audible sound. *Mech. Syst. Signal Process.* **2003**, *17*, 1335–1347. [CrossRef]
14. Langthjem, M.A.; Olhoff, N. A Numerical Study of Flow-Induced Noise in a Two-Dimensional Centrifugal Pump. Part II. Hydroacoustics. *J. Fluids Struct.* **2004**, *19*, 369–386. [CrossRef]
15. Stosiak, M.; Karpenko, M. *Dynamics of Machines and Hydraulic Systems: Mechanical Vibrations and Pressure Pulsations*; Synthesis Lectures on Mechanical Engineering; Springer Nature: Cham, Switzerland, 2024; ISBN 978-3-031-55524-4.
16. Wei, A.; Yu, L.; Qiu, L.; Zhang, X. Cavitation in Cryogenic Fluids: A Critical Research Review. *Phys. Fluids* **2022**, *34*, 101303. [CrossRef]
17. Ge, M.; Petkovšek, M.; Zhang, G.; Jacobs, D.; Coutier-Delgosha, O. Cavitation Dynamics and Thermodynamic Effects at Elevated Temperatures in a Small Venturi Channel. *Int. J. Heat Mass Transf.* **2021**, *170*, 120970. [CrossRef]
18. Franc, J.-P.; Rebattet, C.; Coulon, A. An Experimental Investigation of Thermal Effects in a Cavitating Inducer. *J. Fluids Eng.* **2004**, *126*, 716–723. [CrossRef]
19. Pengo, R.; Junker, S.; Ten Kate, H.H.J. Liquid Helium Centrifugal Pump Characteristics from 80 g/s to 1200 g/s. *Cryogenics* **2010**, *50*, 8–12. [CrossRef]
20. Mihara, S.; Haruyama, T.; Iwamoto, T.; Uchiyama, Y.; Ootani, W.; Kasami, K.; Sawada, R.; Terasawa, K.; Doke, T.; Natori, H.; et al. Development of a Method for Liquid Xenon Purification Using a Cryogenic Centrifugal Pump. *Cryogenics* **2006**, *46*, 688–693. [CrossRef]
21. Haruyama, T.; Mito, T.; Yamamoto, A.; Doi, Y.; Matsumoto, K.; Kajiwara, H. Performance of a Liquid Helium Centrifugal Pump for the TOPAZ Superconducting Magnet. *Cryogenics* **1988**, *28*, 157–160. [CrossRef]

22. Ludtke, P.R.; Daney, D.E. Cavitation Characteristics of a Small Centrifugal Pump in He I and He II. *Cryogenics* **1988**, *28*, 96–100. [CrossRef]
23. Steward, W.G. Centrifugal Pump for Superfluid Helium. *Cryogenics* **1986**, *26*, 97–102. [CrossRef]
24. Li, G.; Caldwell, S.; Clark, J.A.; Gulick, S.; Hecht, A.; Lascar, D.D.; Levand, T.; Morgan, G.; Orford, R.; Savard, G.; et al. A Compact Cryogenic Pump. *Cryogenics* **2016**, *75*, 35–37. [CrossRef]
25. Vaghela, H.; Banerjee, J.; Naik, H.; Sarkar, B. Cryogenic Pump at 4 K Temperature Level -Basic Hydro-Dynamic Design Approach. *Indian J. Cryog.* **2012**, *37*, 134–139.
26. Hou, H.; Zhang, Y.; Li, Z.; Jiang, T.; Zhang, J.; Xu, C. Numerical Analysis of Entropy Production on a LNG Cryogenic Submerged Pump. *J. Nat. Gas Sci. Eng.* **2016**, *36*, 87–96. [CrossRef]
27. Li, W.; Li, S.; Ji, L.; Zhao, X.; Shi, W.; Agarwal, R.K.; Awais, M.; Yang, Y. A Study on the Cavitation and Pressure Pulsation Characteristics in the Impeller of an LNG Submerged Pump. *Machines* **2021**, *10*, 14. [CrossRef]
28. Son, Y.-J.; Kim, Y.-I.; Yang, H.-M.; Lee, K.-Y.; Suh, J.-W.; Yoon, J.Y.; Choi, Y.-S. Influence of Cavitation on Inducer and Return Channels of LNG Pump. *J. Mech. Sci. Technol.* **2024**, *38*, 259–270. [CrossRef]
29. Wang, C.; Zhang, Y.; Hou, H.; Zhang, J.; Xu, C. Entropy Production Diagnostic Analysis of Energy Consumption for Cavitation Flow in a Two-Stage LNG Cryogenic Submerged Pump. *Int. J. Heat Mass Transf.* **2019**, *129*, 342–356. [CrossRef]
30. Zhang, J.; Xu, C.; Zhang, Y.; Zhou, X. Quasi-3D Hydraulic Design in the Application of an LNG Cryogenic Submerged Pump. *J. Nat. Gas Sci. Eng.* **2016**, *29*, 89–100. [CrossRef]
31. Brailovskii, Y.L. High-Pressure Pumps for Cryogenic Liquids: Problems and Prospects. *Chem. Pet. Eng.* **2000**, *36*, 90–93. [CrossRef]
32. Zhang, W.; Gao, R.; Cheng, J.; Chen, W.; Song, Y.; Liao, D. A Review on the Precise Control of the Liquid Nitrogen Supplying System in Transonic Cryogenic Wind Tunnel. *J. Therm. Sci.* **2023**, *32*, 692–707. [CrossRef]
33. Xue, R.; Chen, L.; Zhong, X.; Liu, X.; Chen, S.; Hou, Y. Unsteady Cavitation of Liquid Nitrogen Flow in Spray Nozzles under Fluctuating Conditions. *Cryogenics* **2019**, *97*, 144–148. [CrossRef]
34. Shao, X.; Zhao, W. Liquid Hydrogen Centrifugal Pump Optimization Based on Reducing Hydraulic Loss and Improving Cavitation. *Int. J. Hydrogen Energy* **2024**, *49*, 1419–1431. [CrossRef]
35. Barske, U.M. Development of Some Unconventional Centrifugal Pumps. *Proc. Inst. Mech. Eng.* **1960**, *174*, 437–461. [CrossRef]
36. Watanabe, D.; Manako, H.; Onga, T.; Tamura, T.; Ikeda, K.; Isono, M. Combustion Stability Improvement of LE-9 Engine for Booster Stage of H3 Launch Vehicle. *Mitsubishi Heavy Ind. Tech. Rev.* **2016**, *53*, 28–35.
37. Wang, C.; Xiang, L.; Tan, Y.; Chen, H.; Xu, K. Experimental Investigation of Thermal Effect on Cavitation Characteristics in a Liquid Rocket Engine Turbopump Inducer. *Chin. J. Aeronaut.* **2021**, *34*, 48–57. [CrossRef]
38. Jiang, J.; Li, Y.; Pei, C.; Li, L.; Fu, Y.; Cheng, H.; Sun, Q. Cavitation Performance of High-Speed Centrifugal Pump with Annular Jet and Inducer at Different Temperatures and Void Fractions. *J. Hydrodyn.* **2019**, *31*, 93–101. [CrossRef]
39. Negishi, H.; Ohno, S.; Ogawa, Y.; Aoki, K.; Kobayashi, T.; Okita, K.; Mizuno, T. Numerical Analysis of Unshrouded Impeller Flowfield in the LE-X Liquid Hydrogen Pump. In Proceedings of the 53rd AIAA/SAE/ASEE Joint Propulsion Conference (American Institute of Aeronautics and Astronautics), Atlanta, GA, USA, 10–12 July 2017.
40. Lettieri, C.; Spakovszky, Z.; Jackson, D.; Schwille, J. Characterization of Cavitation Instabilities in a Four-Bladed Turbopump Inducer. *J. Propuls. Power* **2018**, *34*, 510–520. [CrossRef]
41. Gong, Y.; Zhou, F.; Ma, G.; Liu, S. Advancements on Mechanically Driven Two-Phase Cooling Loop Systems for Data Center Free Cooling. *Int. J. Refrig.* **2022**, *138*, 84–96. [CrossRef]
42. Tian, G.; Zhao, C.; Zheng, H.; Fan, X. Experimental Study on the Operating Characteristics of Refrigerant Pumps for Solar Ejector Refrigeration Systems. *Sol. Energy* **2022**, *239*, 50–58. [CrossRef]
43. Zhang, S.; Ma, G.; Zhou, F. Experimental Study on a Pump Driven Loop-Heat Pipe for Data Center Cooling. *J. Energy Eng.* **2015**, *141*, 04014054. [CrossRef]
44. Lin, Y.; Liu, J.; Xu, X.; Liu, Z.; Li, G. Experimental research on air conditioning system of a computer room based on refrigerant pump pressurization. *J. Refrig.* **2020**, *41*, 83–88. (In Chinese)
45. Sun, Y.; Wang, T.; Yang, L.; Hu, L.; Zeng, X. Research of an Integrated Cooling System Consisted of Compression Refrigeration and Pump-Driven Heat Pipe for Data Centers. *Energy Build.* **2019**, *187*, 16–23. [CrossRef]
46. Fang, X.; Zhang, B.; Lin, X.; Zhou, H.; Chen, S.; Hou, Y.; Xue, R.; Zhang, Z. Numerical and Experimental Investigation of Flow Characteristics in a Fluid Self-Lubricating Centrifugal Pump with R134a Refrigerant. *Appl. Sci.* **2023**, *13*, 8062. [CrossRef]
47. Franc, J.-P.; Michel, J.-M. *Fundamentals of Cavitation*; Fluid Mechanics and Its Applications; Springer: Dordrecht, The Netherlands, 2005; Volume 76, ISBN 978-1-4020-2232-6.
48. Ito, Y.; Zheng, X.; Nagasaki, T. One-Way Coupling Numerical Simulation of Cryogenic Cavitation Around an Inducer. *Int. J. Fluid Mach. Syst.* **2019**, *12*, 235–243. [CrossRef]
49. Chen, T.; Mu, Z.; Chen, J.; Tan, S.; Fan, Y. Numerical Investigations on the Mechanisms of the Tip Leakage Vortex Cavitation Development in a Cryogenic Inducer with Large Eddy Simulation. *Phys. Fluids* **2023**, *35*, 073328. [CrossRef]
50. Zhang, Y.; Ren, X.; Wang, Y.; Li, X.; Ito, Y.; Gu, C. Investigation of the Cavitation Model in an Inducer for Water and Liquid Nitrogen. *Proc. Inst. Mech. Eng. Part C J. Mech. Eng. Sci.* **2019**, *233*, 6939–6952. [CrossRef]
51. Ito, Y. The World's First Test Facility That Enables the Experimental Visualization of Cavitation on a Rotating Inducer in Both Cryogenic and Ordinary Fluids. *J. Fluids Eng.* **2021**, *143*, 121105. [CrossRef]

52. Gopalakrishnan, K.; Prentkovskis, O.; Jackiva, I.; Junevičius, R. (Eds.) *TRANSBALTICA XI: Transportation Science and Technology: Proceedings of the International Conference TRANSBALTICA, Vilnius, Lithuania, 2–3 May 2019*; Lecture Notes in Intelligent Transportation and Infrastructure; Springer International Publishing: Cham, Switzerland, 2020; ISBN 978-3-030-38665-8.
53. Shao, X.; Zhao, W. Performance Study on a Partial Emission Cryogenic Circulation Pump with High Head and Small Flow in Various Conditions. *Int. J. Hydrogen Energy* **2019**, *44*, 27141–27150. [CrossRef]
54. Kim, D.-J.; Sung, H.J.; Choi, C.-H.; Kim, J.-S. Cavitation Instabilities of an Inducer in a Cryogenic Pump. *Acta Astronaut.* **2017**, *132*, 19–24. [CrossRef]
55. Kim, D.-J.; Sung, H.J.; Choi, C.-H.; Kim, J.-S. Cavitation Instabilities During the Development Testing of a Liquid Oxygen Pump. *J. Propuls. Power* **2017**, *33*, 187–192. [CrossRef]
56. Shimura, T.; Shimagaki, M.; Watanabe, Y.; Watanabe, M.; Hasegawa, S.; Takata, S. Cavitation induced v ibration of le-7a oxygen turbopump. In Proceedings of the Fifth International Symposium on Cavitation (CAV2003), Osaka, Japan, 1–4 November 2003.
57. Kimura, T.; Yoshida, Y.; Hashimoto, T.; Shimagaki, M. Numerical Simulation for Vortex Structure in a Turbopump Inducer: Close Relationship With Appearance of Cavitation Instabilities. *J. Fluids Eng.* **2008**, *130*, 051104. [CrossRef]
58. Karakas, E.S.; Watanabe, H.; Aureli, M.; Evrensel, C.A. Cavitation Performance of Constant and Variable Pitch Helical Inducers for Centrifugal Pumps: Effect of Inducer Tip Clearance. *J. Fluids Eng.* **2020**, *142*, 021211. [CrossRef]
59. Ge, M.; Zhang, G.; Petkovšek, M.; Long, K.; Coutier-Delgosha, O. Intensity and Regimes Changing of Hydrodynamic Cavitation Considering Temperature Effects. *J. Clean. Prod.* **2022**, *338*, 130470. [CrossRef]
60. Ge, M.; Sun, C.; Zhang, G.; Coutier-Delgosha, O.; Fan, D. Combined Suppression Effects on Hydrodynamic Cavitation Performance in Venturi-Type Reactor for Process Intensification. *Ultrason. Sonochemistry* **2022**, *86*, 106035. [CrossRef] [PubMed]
61. Hord, J. *Cavitation in Liquid Cryogens. 3: Ogives*; NASA: Washington, DC, USA, 1973.
62. Hord, J. *Cavitation in Liquid Cryogens. 4: Combined Correlations for Venturi, Hydrofoil, Ogives, and Pumps*; NASA: Washington, DC, USA, 1974.
63. Ge, M.; Manikkam, P.; Ghossein, J.; Kumar Subramanian, R.; Coutier-Delgosha, O.; Zhang, G. Dynamic Mode Decomposition to Classify Cavitating Flow Regimes Induced by Thermodynamic Effects. *Energy* **2022**, *254*, 124426. [CrossRef]
64. Chen, T.; Huang, B.; Wang, G.; Zhang, H.; Wang, Y. Numerical Investigation of Thermo-Sensitive Cavitating Flows in a Wide Range of Free-Stream Temperatures and Velocities in Fluoroketone. *Int. J. Heat Mass Transf.* **2017**, *112*, 125–136. [CrossRef]
65. Zhang, B.; Zhang, Z.; Fang, X.; Xue, R.; Chen, S.; Hou, Y. Data-Driven Modal Decomposition of R134a Refrigerant Cavitating Flow in Venturi Tube. *Phys. Fluids* **2024**, *36*, 034124. [CrossRef]
66. Chen, T.; Wang, G.; Huang, B.; Wang, K. Numerical Study of Thermodynamic Effects on Liquid Nitrogen Cavitating Flows. *Cryogenics* **2015**, *70*, 21–27. [CrossRef]
67. Long, X.; Liu, Q.; Ji, B.; Lu, Y. Numerical Investigation of Two Typical Cavitation Shedding Dynamics Flow in Liquid Hydrogen with Thermodynamic Effects. *Int. J. Heat Mass Transf.* **2017**, *109*, 879–893. [CrossRef]
68. Chen, T.; Chen, H.; Liang, W.; Huang, B.; Xiang, L. Experimental Investigation of Liquid Nitrogen Cavitating Flows in Converging-Diverging Nozzle with Special Emphasis on Thermal Transition. *Int. J. Heat Mass Transf.* **2019**, *132*, 618–630. [CrossRef]
69. Chen, T.; Chen, H.; Liu, W.; Huang, B.; Wang, G. Unsteady Characteristics of Liquid Nitrogen Cavitating Flows in Different Thermal Cavitation Mode. *Appl. Therm. Eng.* **2019**, *156*, 63–76. [CrossRef]
70. Zhu, J.; Xie, H.; Feng, K.; Zhang, X.; Si, M. Unsteady Cavitation Characteristics of Liquid Nitrogen Flows through Venturi Tube. *Int. J. Heat Mass Transf.* **2017**, *112*, 544–552. [CrossRef]
71. Zhu, J.; Wang, S.; Zhang, X. Influences of Thermal Effects on Cavitation Dynamics in Liquid Nitrogen through Venturi Tube. *Phys. Fluids* **2020**, *32*, 012105. [CrossRef]
72. Murakami, M.; Harada, K. Experimental Study of Thermo-Fluid Dynamic Effect in He II Cavitating Flow. *Cryogenics* **2012**, *52*, 620–628. [CrossRef]
73. Niiyama, K.; Hasegawa, S.; Tsuda, S.; Yoshida, Y.; Tamura, T.; Oike, M. Thermodynamic Effects on Cryogenic Cavitating Flow in an Orifice. In Proceedings of the 7th International Symposium on Cavitation (CAV2009), Ann Arbor, MI, USA, 17–22 August 2009.
74. Liang, W.; Chen, T.; Huang, B.; Wang, G. Thermodynamic Analysis of Unsteady Cavitation Dynamics in Liquid Hydrogen. *Int. J. Heat Mass Transf.* **2019**, *142*, 118470. [CrossRef]
75. Yoshida, Y.; Eguchi, M.; Motomura, T.; Uchiumi, M.; Kure, H.; Maruta, Y. Rotordynamic Forces Acting on Three-Bladed Inducer Under Supersynchronous/Synchronous Rotating Cavitation. *J. Fluids Eng.* **2010**, *132*, 061105. [CrossRef]
76. Yoshida, Y.; Kikuta, K.; Hasegawa, S.; Shimagaki, M.; Tokumasu, T. Thermodynamic Effect on a Cavitating Inducer in Liquid Nitrogen. *J. Fluids Eng.* **2006**, *129*, 273–278. [CrossRef]
77. Ikohagi, T. Influence of Thermodynamic Effect on Synchronous Rotating Cavitation. *J. Fluids Eng.* **2007**, *129*, 871–876.
78. Ito, Y.; Tsunoda, A.; Kurishita, Y.; Kitano, S.; Nagasaki, T. Experimental Visualization of Cryogenic Backflow Vortex Cavitation with Thermodynamic Effects. *J. Propuls. Power* **2016**, *32*, 71–82. [CrossRef]
79. Fan, Y.; Chen, T.; Liang, W.; Wang, G.; Huang, B. Numerical and Theoretical Investigations of the Cavitation Performance and Instability for the Cryogenic Inducer. *Renew. Energy* **2022**, *184*, 291–305. [CrossRef]
80. Chen, Z.; Yang, S.; Li, X.; Li, Y.; Li, L. Investigation on Leakage Vortex Cavitation and Corresponding Enstrophy Characteristics in a Liquid Nitrogen Inducer. *Cryogenics* **2023**, *129*, 103606. [CrossRef]
81. Wei, A.; Wang, W.; Hu, Y.; Feng, S.; Qiu, L.; Zhang, X. Numerical and Experimental Analysis of the Cavitation and Flow Characteristics in Liquid Nitrogen Submersible Pump. *Phys. Fluids* **2024**, *36*, 042109. [CrossRef]

82. Blumenthal, R.F.; Kelecy, F.J. Numerical Predictions of Cavitating Flow Within a Liquid Hydrogen Inducer. In Proceedings of the ASME Turbo Expo 2021: Turbomachinery Technical Conference and Exposition. Volume 2C: Turbomachinery—Design Methods and CFD Modeling for Turbomachinery; Ducts, Noise, and Component Interactions, Virtual, Online, 7–11 June 2021.
83. Challier, G. Thermodynamic Effect on a Cavitating Inducer in Liquid Hydrogen. *J. Fluids Eng.* **2010**, *132*, 111305.
84. Xiang, L.; Tan, Y.; Chen, H.; Xu, K. Numerical Simulation of Cryogenic Cavitating Flow in LRE Oxygen Turbopump Inducer. *Cryogenics* **2022**, *126*, 103540. [CrossRef]
85. Shi, G.; Wei, Y.; Liu, S. Cavitation Flow Characteristics of Water and Liquid Oxygen in the Inducer Considering Thermodynamic Effect. *Energies* **2022**, *15*, 4943. [CrossRef]
86. Holl, J.W.; Billet, M.L.; Weir, D.S. Thermodynamic Effects on Developed Cavitation. *J. Fluids Eng.* **1975**, *97*, 507–513. [CrossRef]
87. Franc, J.-P.; Pellone, C. Analysis of Thermal Effects in a Cavitating Inducer Using Rayleigh Equation. *J. Fluids Eng.* **2007**, *129*, 974–983. [CrossRef]
88. Ren, T. Study on the High Speed Motorized Centrifugal Air Compressor with Water Lubricated Journal Bearing. Ph.D. Thesis, University of Science and Technology Beijing, Beijing, China, 2017. (In Chinese)
89. Wu, C. Investigation of Low-Specific-Speed Centrifugal Impeller Fluid-Induced Excitations and Its Control Methods. Ph.D. Thesis, Zhejiang University, Hangzhou, China, 2023. (In Chinese)